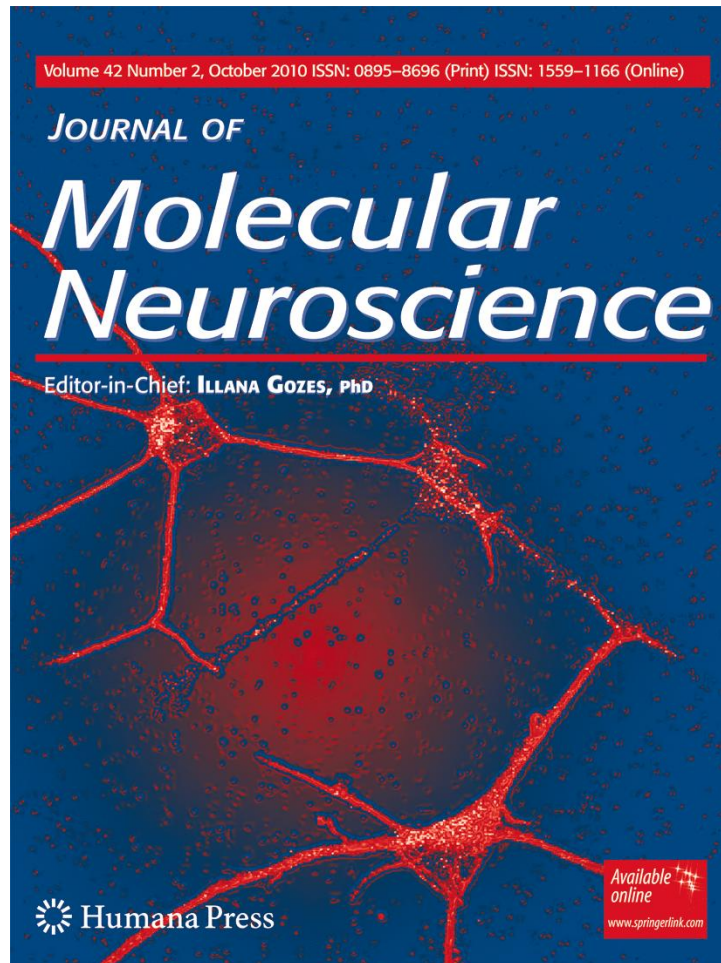


ISSN 0895-8696, Volume 42, Number 2



**This article was published in the above mentioned Springer issue.
The material, including all portions thereof, is protected by copyright;
all rights are held exclusively by Springer Science + Business Media.
The material is for personal use only;
commercial use is not permitted.
Unauthorized reproduction, transfer and/or use
may be a violation of criminal as well as civil law.**

Influence of Chronic Nicotine Administration on Cerebral Type 1 Cannabinoid Receptor Binding: An In Vivo Micro-PET Study in the Rat Using [¹⁸F]MK-9470

Nathalie Gérard · Jenny Ceccarini · Guy Bormans · Bert Vanbilloen · Cindy Casteels · Karolien Goffin · Barbara Bosier · Didier M. Lambert · Koen Van Laere

Received: 8 January 2010 / Accepted: 4 February 2010 / Published online: 25 February 2010
© Springer Science+Business Media, LLC 2010

Abstract Several lines of evidence suggest a functional interaction between central nicotinic and endocannabinoid systems. Furthermore, type 1 cannabinoid receptor (CB1R) antagonism is evaluated as antismoking therapy, and nicotine usage can be an important confound in positron emission tomography (PET) imaging studies of the CB1R. We evaluated CB1R binding in the rat brain using the PET radioligand [¹⁸F]MK-9470 after chronic administration of nicotine. Twelve female Wistar rats were scanned at baseline and after chronic administration of either nicotine (1 mg/kg; 2 weeks daily intraperitoneal (IP)) or saline as control. In vivo micro-PET images of CB1R binding were anatomically standardized and analyzed by voxel-based

statistical parametric mapping and a predefined volume-of-interest approach. We did not observe changes in [¹⁸F]MK-9470 binding ($p_{\text{height}} < 0.001$ level; uncorrected) on a group basis in either condition. Only at a less stringent threshold of $p_{\text{height}} < 0.005$ (uncorrected) was a modest increase observed in tracer binding in the cerebellum for nicotine (peak voxel value + 6.8%, $p_{\text{cluster}} = 0.002$ corrected). In conclusion, chronic IP administration of nicotine does not produce major cerebral changes in CB1R binding of [¹⁸F]MK-9470 in the rat. These results also suggest that chronic nicotine usage is unlikely to interfere with human PET imaging using this radioligand.

Keywords Nicotine · Type 1 cannabinoid receptor · Micro-PET · Rat brain

N. Gérard (✉) · J. Ceccarini · B. Vanbilloen · C. Casteels · K. Goffin · K. Van Laere
Division of Nuclear Medicine, E901,
Catholic University Leuven and University Hospitals Leuven,
Herestraat 49,
3000 Leuven, Belgium
e-mail: nathalie.gerard@uzleuven.be

N. Gérard · J. Ceccarini · C. Casteels · K. Goffin · K. Van Laere
Molecular Small Animal Imaging Center (MOSAIC),
Catholic University Leuven,
O&N 1, Herestraat 49 bus 505,
3000 Leuven, Belgium

G. Bormans
Laboratory for Radiopharmacy, Catholic University Leuven,
O&N 2, Herestraat 49 bus 821,
3000 Leuven, Belgium

B. Bosier · D. M. Lambert
Unité de Chimie Pharmaceutique et de Radiopharmacie,
Université Catholique de Louvain,
Avenue Mounier 73.40,
1200 Brussels, Belgium

Introduction

Nicotine is considered to be the primary psychoactive compound of tobacco smoke that establishes and maintains tobacco dependence. Several lines of evidence suggest that there may be a functional interaction between the central nicotinic and endocannabinoid systems (ECS; Castane et al. 2005). The ECS is involved in the brain reward processing circuitry which becomes activated in drug addiction. Release of endocannabinoids in the ventral tegmental area (VTA), an important component of the reward and mesocorticolimbic dopaminergic circuitry, is assumed to play a role in inducing the rewarding effects of multiple drugs and may contribute to a common mechanism of addiction (Maldonado et al. 2006). The VTA also contains many nicotinic acetylcholine receptors (nAChR) by which nicotine triggers mesolimbic dopamine release (Dani et al. 2005).

The ECS has been studied extensively since the characterization of a specific G-protein-coupled cannabinoid receptor in the rat brain (Devane et al. 1988). This type 1 cannabinoid receptor (CB1R) is expressed in high concentrations in the brain and is preferentially distributed at presynaptic neurons where it modulates the central effects of cannabis and cannabinoid drugs and exerts its effects by inhibition of the release of other neurotransmitters, e.g., γ -aminobutyric acid, glutamate, and dopamine. A second cannabinoid receptor, CB2, exists but is mainly expressed in peripheral tissues, especially in cells of the immune system. Different endogenous ligands, or endocannabinoids, are known for these receptors. Anandamide (AEA) and 2-arachidonoyl glycerol (2-AG) are the two best characterized endogenous agonists (Di Marzo et al. 2004).

The association between cannabis and nicotine abuse is known in humans through epidemiological, pharmacological, and behavioral studies (Viveros et al. 2006). In rats, nicotine and endocannabinoids seem to enhance the reinforcing effects of both systems (Viveros et al. 2006), and changes in endogenous cannabinoid levels have been observed in different brain regions chronically exposed to nicotine, such as the brainstem, hippocampus, cerebral cortex, and striatum (Gonzalez et al. 2002). In mice, administration of nicotine facilitates the pharmacological responses, tolerance, and physical dependence induced by Δ^9 -tetrahydrocannabinol (THC), the major psychoactive component of *Cannabis sativa* (Valjent et al. 2002).

The CB1R may have an important role in the interplay between the nicotinic system and the ECS. This receptor is abundantly expressed in the cerebellum and in important reward circuitry components among which are the VTA, nucleus accumbens, amygdala, and hippocampus (Herkenham et al. 1990). The rewarding effect of nicotine is reduced in CB1R knockout mice (Castane et al. 2002), while CB1R antagonists are able to reduce nicotine addiction, in rats but also in humans (Cohen et al. 2002; Siu et al. 2007). In a self-administration and a place conditioning paradigm in rats, it has been shown that pretreatment with the CB1R inverse agonist rimonabant decreased the response on the lever to obtain intravenous nicotine infusions and the expression of a conditioned place preference associated to nicotine, respectively (Cohen et al. 2005).

In the present study, we evaluated possible alterations in CB1R binding in the rat brain after daily chronic administration of nicotine, using small-animal positron emission tomography (PET) imaging and [^{18}F]MK-9470 (*N*-[2-(3-cyano-phenyl)-3-(4-(2-[^{18}F]fluoroethoxy) phenyl)-1-methylpropyl]-2-(5-methyl-2-pyridyloxy)-2-methyl propanamide), a subtype-selective and high-affinity radioligand for the CB1R (Burns et al. 2007). The primary objective was to quantify potential direct pharmacological interactions between nicotine and CB1R availability from a pathophysi-

ological viewpoint and assess potential bias by subject smoking in human imaging studies (Van Laere et al. 2008).

Materials and Methods

Direct Binding Affinity

Direct binding affinity of nicotine at the CB1R was evaluated in vitro using a competitive binding assay, as previously described (Govaerts et al. 2004). Experiments were conducted on membrane preparation from human CB1R-transfected Chinese hamster ovarian cells (CHO-CB1) incubated with 1 nM [^3H]-SR141716A (Amersham, Roosendaal, The Netherlands) and appropriate concentration of competition ligand. Nonspecific binding was determined in the presence of 10 μM of the potent cannabinoid agonist HU 210 ((+)-1,1-dimethylheptyl analog of 7-hydroxy- Δ^6 -tetrahydrocannabinol; Tocris Cookson, Bristol, UK).

Micro-PET Imaging

Twelve female Wistar rats (body weight range 206–323 g; age 12 weeks; Charles River Laboratories France) were housed three to a cage with food and water freely accessible in a 12-h dark–light cycle (lights on from 8 a.m. to 8 p.m. daily). The research protocol was approved by the local Animal Ethics Committee and was according to the European Ethics Committee guidelines (decree 86/609/EEC).

To induce the chronic condition, animals received a daily intraperitoneal (IP) nicotine ($n=6$, 1 mg/kg, 1 ml) or 0.9% saline ($n=6$, 1 ml) injection for 2 weeks. (–)-Nicotine hydrogen tartrate salt (purity grade $\geq 98\%$, Sigma-Aldrich, N5260) was used, dissolved in 0.9% saline. The saline-treated rat data were used from similar pharmacological interaction studies (Goffin et al. 2008; Casteels et al. 2010). The dosage was chosen according to previous experiments and its ability to affect endocannabinoid transmission (Miksys et al. 2000; Gonzalez et al. 2002).

The precursor for [^{18}F]MK-9470 was obtained from Merck Research Laboratories (MRL, West Point, USA), and labeling was performed by alkylation of the precursor with 2-[^{18}F]fluoroethyl bromide. Tracer preparation and characteristics have been described previously (Burns et al. 2007).

Animals were anesthetized for scanning with an IP injection of 50 mg/kg sodium pentobarbital (Nembutal[®], CEVA Santé Animale, Brussels, Belgium). All rats were fasted for at least 6 h prior to tracer administration and PET imaging. An 18 MBq (500 μCi ; mean = 519 ± 118 μCi ; injection volume 500 μL) [^{18}F]MK-9470 radioligand was administered via a tail vein. Specific activity of the tracer

was always higher than 10 GBq/ μmol at injection time. Animals were imaged on day 1 in baseline condition and on day 15 following daily nicotine or saline injections.

Small-animal PET imaging was performed on a Concorde Focus 220 micro-PET (Siemens/Concorde Microsystems, Knoxville, TN, USA) which has a transaxial resolution of 1.35 mm full width at half maximum. All data were acquired in list mode in a $128 \times 128 \times 95$ matrix with a pixel width of 0.475 mm and a slice thickness of 0.796 mm. Images were acquired dynamically for 60 min immediately following tracer injection.

Scans were reconstructed using filtered back projection, and the last 20 min was used for measurement of radioactivity concentration and quantification. As previously described (Casteels et al. 2006), all micro-PET images were coregistered and spatially normalized to a stereotactic space based upon the rat brain Paxinos atlas (Paxinos et al. 1998). [^{18}F]MK-9470 binding was estimated using parametric images based on standardized uptake values (SUV), a unitless measure used to correct for differences in injected dose and subject body weight, making comparisons between subjects possible ($\text{SUV} = \text{activity concentration (MBq/ml)} \times \text{subject's weight (g)} / \text{injected dose (MBq)}$; Burns et al. 2007).

Predefined volume-of-interest (VOI) and voxel-based statistical parametric mapping (SPM2, Wellcome Department of Imaging Neuroscience, London, UK) analyses were performed. For VOI analysis, a predefined VOI map was loaded on all parametric images to permit calculation of average SUVs within each VOI as shown in Fig. 2 (PMOD software, version 2.65; PMOD Inc., Zurich, Switzerland). The differences of chronic and baseline SUV data (SUV_{diff}) were calculated for both groups [$((\text{CHR} - \text{BL}) \times 2) / (\text{CHR} + \text{BL})$], and these values were compared with a Mann–Whitney U test (nonparametric analysis of variance). Also, a univariate analysis was done by comparing chronic to baseline SUV data within each group with nonparametric Wilcoxon matched-pairs tests (Statistica, version 6.1; StatSoft Inc., Tulsa,

OK, USA). Comparisons resulting in p values below 0.05 were considered significant.

For SPM analysis, data were smoothed with an isotropic Gaussian kernel of 1.2 mm full width at half maximum. Only significant clusters ($p < 0.05$, corrected for multiple comparisons) were retained, in combination with sufficient localizing power ($p_{\text{height}} < 0.005$, uncorrected for multiple comparisons). The extent threshold k_{ext} was higher than 200 voxels (Casteels et al. 2006). For analysis of relative receptor binding, activity normalization was done on total cerebral counts using proportional scaling, and a relative (gray matter) analysis threshold of 80% was set to exclude extracerebral activity.

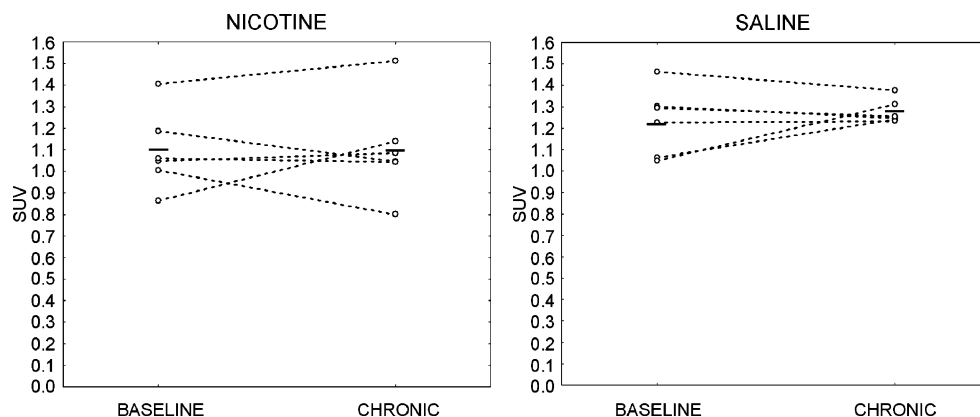
Results

A competitive binding assay demonstrated that the in vitro direct binding affinity of nicotine at the CB1R was negligible. Ligand displacement was $23.9 \pm 0.1\%$ (mean \pm SD) and $21.7 \pm 1.3\%$ at 10 and 100 μM nicotine, respectively, which implies that the IC_{50} for nicotine is higher than 100 μM .

The changes in [^{18}F]MK-9470 binding between the baseline and chronic condition, expressed as SUV_{diff} values, were compared between the nicotine and the control groups. No significant differences were found in SUV_{diff} values of the nicotine and control group. The absolute mean cerebral SUV_{diff} was 0.002 for the nicotine group and 0.042 for the sham group ($p = 0.94$).

In a univariate analysis, chronic saline injections did not produce any significant changes in [^{18}F]MK-9470 binding within this control group. The mean SUV value within the cerebral VOI at baseline was 1.23 and 1.28 after 2 weeks of saline administration ($p = 0.47$; Fig. 1). In the nicotine-treated rats, also no absolute changes in [^{18}F]MK-9470 binding were found on a group basis (Fig. 1). The intersubject variability (expressed as coefficient of variation per VOI) of the absolute baseline measurements in both

Figure 1 Scatter plot of the mean global gray matter (all volume-of-interest regions) standardized uptake values (SUV) versus condition for the six nicotine-treated rats (left) and the six control (saline-treated) rats (right). Horizontal lines indicate the mean SUV in each condition



groups ranged from 5% to 20% (average coefficient of variation = 14.8%).

Exploring regional changes within the nicotine group, SPM analysis of relative [^{18}F]MK-9470 binding showed a small but significant increase in the chronic condition compared to baseline in a cluster located in the left and middle (vermis) cerebellum (Figs. 2 and 3). The peak voxel difference was +6.8% ($p_{\text{height}} < 0.005$ uncorrected, $p_{\text{cluster}} = 0.002$ corrected) and located at Paxinos coordinates $x = -2.8$ mm, $y = -14.2$ mm, $z = -3.4$ mm (x = lateral distance from the brain midline; y = anteroposterior location relative to Bregma; z = dorsoventral position; Table 1). VOI analysis confirmed this finding with a significant relative increase of average radioligand binding in a region of the (bilateral) cerebellar volume of interest (125 mm 3) of 1.8% ($p = 0.041$). No other areas of significant changes were found on predefined VOI analysis.

Discussion

To our knowledge, *in vivo* data of CB1 receptor availability changes due to nicotine exposure have not been previously reported. *Ex vivo* studies showed an almost complete lack of changes in mRNA levels or binding capacity of CB1R following chronic nicotine exposure (Gonzalez et al. 2002; Balerio et al. 2004). Gonzalez et al. found an increase in endocannabinoid levels (AEA and/or 2-AG) in the limbic forebrain and brainstem, while the hippocampus, cerebral cortex, and striatum exhibited a decrease in endocannabinoid levels. No changes were seen in the cerebellum. In contrast, significant changes in CB1 receptor protein levels, quantified by Western blotting, were reported by Marco et al. (2007). They observed increased hippocampal CB1R

expression and decreased striatal CB1R expression after 10 days of nicotine treatment, albeit in adolescent rats and after a posttreatment interval of a month. In addition to the evidence for increased effects of cannabinoids in adolescent animals, the same may be true for nicotine. Nicotine in adolescent, but not in adult male rats, produced changes in cannabinoid receptors in specific brain regions (Werling et al. 2009).

In the present study, the absolute SUV changes in the nicotine group were not significantly different from the changes observed after saline treatment. We found a modest univariate increase of regional cerebellar CB1R binding following chronic nicotine exposure. This change is unlikely to result from a direct nicotinic effect onto the CB1R, as we found no significant affinity of nicotine at these receptors ($\text{IC}_{50} > 100$ μM), implying nicotine itself is unable to displace the high-affinity [^{18}F]MK-9470 radioligand (rat $\text{IC}_{50} = 0.9$ nM) at the used dosage. As nicotine has a half-life of 45 min in rat plasma, the last dose—administered 24 h before the scan—was eliminated at the time of PET scanning.

Therefore, indirect effects of chronic nicotine administration on the ECS are most likely responsible for the observed change by either modulation of endocannabinoids or modulation of CB1 receptor density and/or affinity. Previous studies have indicated that nicotine regionally influences levels of endocannabinoids (Gonzalez et al. 2002; Maldonado et al. 2006; Marco et al. 2007) and increases in anandamide can induce changes in cerebellar CB1 receptor binding, probably through changes in receptor density (Romero et al. 1995). After chronic exposure to this endogenous agonist, the binding capacity of CB1 receptors in the cerebellum and hippocampus increases, while these receptors remained unaffected in other brain regions (Romero et al. 1995). Other findings also support this regional dependence of cannabinoid receptor response to agonists, such as the regionally and treatment-dependent CB1R downregulation elicited by administration of the exogenous CB1R agonists THC and WIN 55,212-2 (Sim-Selley et al. 2002).

The cerebellum is a brain region with a high density of CB1 receptors and nicotinic acetylcholine receptors, the latter mostly containing $\alpha 7$ or $\alpha 4$ and $\beta 2$ subunits (Herkenham et al. 1990; Reno et al. 2004). By stimulating $\alpha 7$ -nAChRs, nicotine induces enhanced glutamate release, resulting in increased cerebellar oxidative stress (Reno et al. 2004). It can be hypothesized that, in view of the homeostatic nature of the endocannabinoid system and its ability to downregulate cerebellar glutamate release (Breivogel et al. 2004), the obtained CB1R upregulation could be an attempt to counteract this increased glutamatergic neurotransmission and reestablish baseline neurotransmission levels.

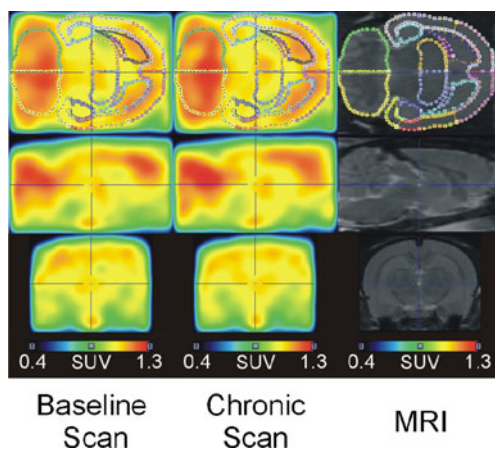


Figure 2 Micro-PET mean images of nicotine-treated rats visualizing [^{18}F]MK-9470 binding per condition expressed in standardized uptake values (SUV). The spatially normalized MRI template and the overlaid volume-of-interest map are shown in the *right column* and *upper row*, respectively

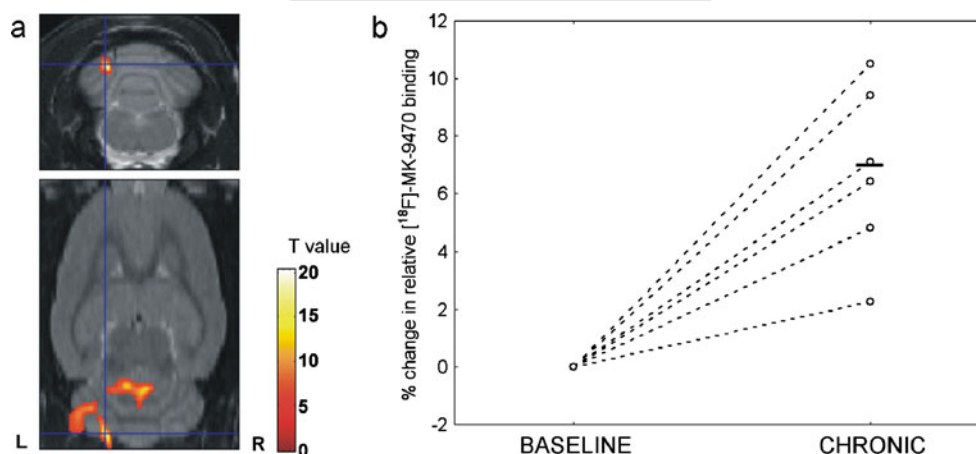


Figure 3 **a** Orthogonal section with SPM T-map for the relative difference in $[^{18}\text{F}]$ MK-9470 binding after chronic nicotine injection rendered on the MRI atlas of the rat brain in Paxinos space (L = left; R = right). T values are indicated by the color bar. **b** Change (in

percentage) of the relative standardized uptake values (SUV) at the maximal peak location in the cerebellum after chronic nicotine administration for each rat. The mean value of increase in the chronic condition is indicated by the horizontal line

The area-under-the-curve SUV macroparameter is a good index of CB1R binding at the measured scanning interval, as indicated by modeling studies of tracer kinetics (Burns et al. 2007; Sanabria-Bohórquez et al. 2010; Terry et al. 2009). Possible increases in regional cerebral blood flow (CBF) induced by nicotine as documented by brain imaging studies in humans (Rose et al. 2007) could theoretically augment the tracer delivery to the brain. We have empirically observed only minimal effects of CBF changes on the SUV macroparameter using IV acetazolamide at concentrations that induce up to 70% CBF increases in the rat brain (unpublished results). Therefore, possible CBF changes are unlikely to have confounded our results.

Nicotine-treated animals show a higher intersubject variability in CB1R availability measurements compared to saline-treated animals, at baseline as well as after the treatment period. Possible reasons for this cannot be obviously inferred from this experiment; however, some factors should be taken into consideration. Firstly, despite

all animals being female, it is possible that the hormonal status of the animals differs between both groups and that this difference influences radioligand uptake. Secondly, data from the saline rats, as a historical control group, were acquired in an identical experimental setting but at a different time. Finally, increasing the number of subjects per group could be a way to reduce intersubject variability in future studies.

As this study has only addressed the pharmacological effect of nicotine administration on $[^{18}\text{F}]$ MK-9470 binding at the CB1R and rewarding effects of smoking are not fully reproducible in this animal model, our results do not exclude a possible role of the CB1R and ECS in tobacco-induced nicotine addiction.

In conclusion, administration of nicotine does not alter the in vivo CB1R availability in the rat cerebrum measured with $[^{18}\text{F}]$ MK-9470, and only a modest regional CB1R binding increase was found in the cerebellum. From a translational point of view, this study suggests that chronic

Table 1 p values and locations of the significant clusters in the comparison of the relative CB1R availability in the chronic condition versus the baseline condition in nicotine-treated rats

Chronic > baseline								
Cluster level			Voxel level			Structure		
p_{corr}	k_E	p_{uncorr}	T	p_{uncorr}	x	y	z	
0.002	591	<0.0001	14.94	<0.005	-2.8	-14.2	-3.4	Left cerebellar hemisphere
			11.64	<0.005	-3.2	-13.2	-4.0	
			11.63	<0.005	-5.2	-12.6	-4.0	

k_E cluster extent, x lateral distance in millimeter from the midline (a negative value indicates a localization on the left side), y anteroposterior location relative to Bregma (negative values indicate spots posterior to Bregma), z dorsoventral position (based upon the Paxinos stereotactic atlas)

nicotine usage is unlikely to interfere with in vivo CB1R binding of [¹⁸F]MK-9470 in human studies, although direct confirmation in humans is needed.

Acknowledgements Merck & Co, Inc. is acknowledged for the availability of the precursor of [¹⁸F]MK-9470. The authors thank Mr. Peter Vermaelen for his assistance in the animal work and the Leuven PET radiopharmacy team for tracer preparations. This work was supported by the Research Council of K.U. Leuven (OT/05/58). KG is supported by a research mandate of the Flemish Fund for Scientific Research. KVL is a Senior Clinical Investigator of the Flemish Fund for Scientific Research. The authors have no conflicts of interest to declare.

References

- Balerio GN, Aso E, Berrendero F, Murtra P, Maldonado R (2004) Delta9-tetrahydrocannabinol decreases somatic and motivational manifestations of nicotine withdrawal in mice. *Eur J Neurosci* 20:2737–2748
- Breivogel CS, Walker JM, Huang SM, Roy MB, Childers SR (2004) Cannabinoid signaling in rat cerebellar granule cells: G-protein activation, inhibition of glutamate release and endogenous cannabinoids. *Neuropharmacology* 47:81–91
- Burns HD, Van Laere K, Sanabria-Bohorquez S et al (2007) [¹⁸F]MK-9470, a positron emission tomography (PET) tracer for in vivo human PET brain imaging of the cannabinoid-1 receptor. *Proc Natl Acad Sci U S A* 104:9800–9805
- Castane A, Valjent E, Ledent C, Parmentier M, Maldonado R, Valverde O (2002) Lack of CB1 cannabinoid receptors modifies nicotine behavioural responses, but not nicotine abstinence. *Neuropharmacology* 43:857–867
- Castane A, Berrendero F, Maldonado R (2005) The role of the cannabinoid system in nicotine addiction. *Pharmacol Biochem Behav* 81:381–386
- Casteels C, Vermaelen P, Nuyts J et al (2006) Construction and evaluation of multitracer small-animal PET probabilistic atlases for voxel-based functional mapping of the rat brain. *J Nucl Med* 47:1858–1866
- Casteels C, Vanbilloen B, Vercammen D et al (2010) Influence of chronic bromocriptine and levodopa administration on cerebral type 1 cannabinoid receptor binding. *Synapse* (in press)
- Cohen C, Perrault G, Voltz C, Steinberg R, Soubrie P (2002) SR141716, a central cannabinoid (CB1) receptor antagonist, blocks the motivational and dopamine-releasing effects of nicotine in rats. *Behav Pharmacol* 13:451–463
- Cohen C, Kudas E, Griebel G (2005) CB1 receptor antagonists for the treatment of nicotine addiction. *Pharmacol Biochem Behav* 81:387–395
- Dani JA, Harris RA (2005) Nicotine addiction and comorbidity with alcohol abuse and mental illness. *Nat Neurosci* 8:1465–1470
- Devane WA, Dysarz FAI, Johnson MR, Melvin LS, Howlett AC (1988) Determination and characterization of a cannabinoid receptor in rat brain. *Mol Pharmacol* 34:605–613
- Di Marzo V, Bifulco M, De Petrocellis L (2004) The endocannabinoid system and its therapeutic exploitation. *Nat Rev Drug Discov* 3:771–784
- Goffin K, Bormans G, Casteels C et al (2008) An in vivo [¹⁸F]MK-9470 micro-PET study of type 1 cannabinoid receptor binding in Wistar rats after chronic administration of valproate and levetiracetam. *Neuropharmacology* 54:1103–1106
- Gonzalez S, Cascio MG, Fernandez-Ruiz J, Fezza F, Di Marzo V, Ramos JA (2002) Changes in endocannabinoid contents in the brain of rats chronically exposed to nicotine, ethanol or cocaine. *Brain Res* 954:73–81
- Govaerts SJ, Hermans E, Lambert DM (2004) Comparison of cannabinoid ligands affinities and efficacies in murine tissues and in transfected cells expressing human recombinant cannabinoid receptors. *Eur J Pharm Sci* 23:233–243
- Herkenham M, Lynn AB, Little MD et al (1990) Cannabinoid receptor localization in brain. *Proc Natl Acad Sci U S A* 87:1932–1936
- Maldonado R, Valverde O, Berrendero F (2006) Involvement of the endocannabinoid system in drug addiction. *Trends Neurosci* 29:225–232
- Marco EM, Granstrem O, Moreno E et al (2007) Subchronic nicotine exposure in adolescence induces long-term effects on hippocampal and striatal cannabinoid-CB1 and mu-opioid receptors in rats. *Eur J Pharmacol* 557:37–43
- Miksys S, Hoffmann E, Tyndale RF (2000) Regional and cellular induction of nicotine-metabolizing CYP2B1 in rat brain by chronic nicotine treatment. *Biochem Pharmacol* 59:1501–1511
- Paxinos G, Watson C (1998) The rat brain in stereotaxic coordinates. Academic, Orlando
- Reno LA, Zago W, Markus RP (2004) Release of [(3)H]-L-glutamate by stimulation of nicotinic acetylcholine receptors in rat cerebellar slices. *Neuroscience* 124:647–653
- Romero J, Garcia L, Fernandez-Ruiz JJ, Cebeira M, Ramos JA (1995) Changes in rat brain cannabinoid binding sites after acute or chronic exposure to their endogenous agonist, anandamide, or to delta 9-tetrahydrocannabinol. *Pharmacol Biochem Behav* 51:731–737
- Rose JE, Behm FM, Salley AN et al (2007) Regional brain activity correlates of nicotine dependence. *Neuropsychopharmacology* 32:2441–2452
- Sanabria-Bohórquez SM, Hamill TG, Goffin K et al (2010) Kinetic analysis of the cannabinoid-1 receptor PET Tracer [¹⁸F]MK-9470 in human brain. *Eur J Nucl Med Mol Imaging* (in press)
- Sim-Selley LJ, Martin BR (2002) Effect of chronic administration of R-(+)-[2,3-dihydro-5-methyl-3-[(morpholinyl)methyl]pyrrolo[1, 2, 3-de]-1, 4-benzoxazinyl]-(1-naphthalenyl)methanone mesylate (WIN55, 212–2) or delta(9)-tetrahydrocannabinol on cannabinoid receptor adaptation in mice. *J Pharmacol Exp Ther* 303:36–44
- Siu EC, Tyndale RF (2007) Non-nicotinic therapies for smoking cessation. *Annu Rev Pharmacol Toxicol* 47:541–564
- Terry GE, Liow JS, Zoghbi SS et al (2009) Quantitation of cannabinoid CB1 receptors in healthy human brain using positron emission tomography and an inverse agonist radioligand. *Neuroimage* 48:362–370
- Valjent E, Mitchell JM, Besson MJ, Caboche J, Maldonado R (2002) Behavioural and biochemical evidence for interactions between delta 9-tetrahydrocannabinol and nicotine. *Br J Pharmacol* 135:564–578
- Van Laere K, Goffin K, Casteels C et al (2008) Gender-dependent increases with healthy aging of the human cerebral cannabinoid-type 1 receptor binding using [(18)F]MK-9470 PET. *Neuroimage* 39:1533–1541
- Viveros MP, Marco EM, File SE (2006) Nicotine and cannabinoids: parallels, contrasts and interactions. *Neurosci Biobehav Rev* 30:1161–1181
- Werling LL, Reed SC, Wade D, Izenwasser S (2009) Chronic nicotine alters cannabinoid-mediated locomotor activity and receptor density in periadolescent but not adult male rats. *Int J Dev Neurosci* 27:263–269